Critical Thickness for Antiferroelectricity in $PbZrO_3$

B. K. Mani,[1] C.-M. Chang,[1,2] S. Lisenkov,[1] and I. Ponomareva[1]
[1]Department of Physics, University of South Florida, Tampa, Florida 33620, USA
[2]Institute for Cyber-Enabled Research, Michigan State University, Biomedical & Physical Sciences Building, 567 Wilson Road, Room 1440, East Lansing, Michigan 48824-1226, USA

(Received 1 May 2015; published 26 August 2015; corrected 21 December 2015)

Ferroelectrics and antiferroelectrics appear to have just the opposite behavior upon scaling down. Below a critical thickness of just a few nanometers the ferroelectric phase breaks into nanodomains that mimic electric properties of antiferroelectrics very closely. On the other hand, antiferroelectric thin films were found to transition from the antiferroelectric behavior to a ferroelectric one under certain growth conditions. At present, the origin of such a transition is controversial. Here, we use accurate first-principles-based finite-temperature simulations to predict the existence of a critical thickness for antiferroelectricity in the most celebrated antiferroelectric, $PbZrO_3$. The origin of this effect is traced to the intrinsic surface contribution that has been previously overlooked. The existence of a critical thickness below which the antiferroelectric phase is replaced with a ferroelectric one not only complements the discovery of a critical thickness for ferroelectricity, but also suggests that ferroelectricity and antiferroelectricity are just two opposite manifestations of the same phenomenon: the material's tendency to develop a long-range order. Nanoscaling offers the opportunity to manipulate this order.

DOI: 10.1103/PhysRevLett.115.097601 PACS numbers: 77.80.-e, 77.55.fp, 77.55.Px

Ferroelectrics are the materials that possess spontaneous polarization that can be reversed by the application of an external electric field. Antiferroelectrics are often considered to be antipolar counterparts of ferroelectrics as they can transition into a polar "ferroelectric-like" phase under an applied electric field. Both ferroelectrics and antiferroelectrics find numerous practical applications and are very promising for miniaturized devices. Interestingly, ferroelectrics and antiferroelectrics exhibit nearly opposite behavior upon scaling down. The nanoscale behavior of ferroelectrics is largely governed by the depolarizing field that affects most of their electric properties including the ferroelectric phase itself [1–3]. Indeed, it was first predicted that the ferroelectricity disappears below a critical thickness of 2.4 nm [2]. However, it was soon realized that, in such ultrathin films, the spontaneous polarization does not disappear altogether but, rather, forms nanodomains which annihilate the depolarizing field [3,4]. Interestingly, such nanodomain structures can be considered to be an antipolar, or "antiferroelectric-like," phase of a ferroelectric material as they exhibit double hysteresis loops typical of antiferroelectrics [5,6]. On the other hand, antiferroelectrics appear to demonstrate just the opposite behavior upon scaling down. More precisely, they were reported to develop a ferroelectric phase at the nanoscale [7–11]. It seems that the effects that arise at the nanoscale are capable of inducing a transition between the polar and antipolar phases of the same material.

Interestingly, while the transition from a polar to an antipolar phase in ferroelectric thin films is well investigated and understood [3,4,12,13], the antipolar-to-polar transition in nanoscale antiferroelectrics remains rather puzzling. Ref. [9] reported that $PbZrO_3$ films with thickness less than 22 nm show a ferroelectric-like hysteresis loop. It was proposed that the epitaxial strain stabilizes the ferroelectric (FE) phase. Interestingly, polycrystalline $PbZrO_3$ films exhibit FE-like single loop hysteresis at a larger thickness of 80 nm [8]. The thickness dependent behavior of the polycrystalline films was tentatively attributed to the interface layer between the film and electrode. The possibility of stabilizing the FE phase in $PbZrO_3$ by epitaxial compressive strain at zero Kelvin was later established in first principles simulations [11]. At the same time, the epitaxial strain effects cannot explain one of the earliest experimental reports of a size-driven antiferroelectric-ferroelectric (AFE-FE) transition in $PbZrO_3$ films and $BiNbO_4$ films [7]. The coexistence of FE and AFE phases was also observed in $PbZrO_3$ films [14]. A transition from a mixed AFE-FE behavior to a FE behavior was reported in $PbZrO_3/Pb(Zr_{0.8}Ti_{0.2})O_3$ multilayers with a thickness of $PbZrO_3$ layer below 10 nm [10]. This effect was attributed to the epitaxial strain.

In this Letter, we take advantage of accurate first-principles-based finite-temperature simulations to (i) predict the existence of a critical thickness for antiferroelectricity in $PbZrO_3$ ultrathin films, including the unstrained films, (ii) reveal an overlooked surface effect that triggers the size-driven AFE-FE transition in such ultrathin films, (iii) outline how the proposed mechanism could reconcile many of the aforementioned controversies and address some of the open questions, and (iv) decouple the contributions from the surface effect, residual depolarizing field, and epitaxial strain to the phase formation and electric properties of ultrathin $PbZrO_3$ films.

$PbZrO_3$ ultrathin films grown along a [001] pseudocubic direction (z-Cartesian axis in our case) and of 1.6 to 8.3 nm

thicknesses are simulated using $12 \times 12 \times N$ supercells that are periodic along the films in-plane directions (x- and y-Cartesian axes in our case). N represents the number of unit cells along the film's growth direction and ranges from 4 to 20. The energy of the supercell is given by the first-principles effective Hamiltonian [15,16] for $PbZrO_3$ [17]. The degrees of freedom for the Hamiltonian include local modes, $\mathbf{u}_i$, that are proportional to the dipole moment in the unit cell, i, oxygen octahedron tilts about pseudocubic axes, $\boldsymbol{\omega}_i$, that describe oxygen octahedron rotation, and strain variable tensors (in Voigt notations), η_i, that are responsible for mechanical deformations of a unit cell. Note that the unit cell, here, refers to a five atom cell of cubic perovskite. The energy of the $PbZrO_3$ Hamiltonian includes dipole-dipole interactions, short-range interaction, on-site self-energies, elastic energy, coupling between the degrees of freedom, and the interaction between the local modes and the electric field. The Hamiltonian correctly reproduces many electrical and thermodynamical properties of $PbZrO_3$. In particular, it accurately predicts the antiferroelectric phase transition and the dipole pattern associated with it, electric hysteresis loops, and $PbZrO_3$ behavior under pressure. The Curie point of 946 K, however, overestimates the experimental value of 503 K. It should be noted that the effective Hamiltonian approach has been widely used to predict numerous properties of ferroelectrics, multiferroics, and related materials [18–22]. The energy given by the Hamiltonian is used in Monte Carlo simulations. Typically, 40 000 Monte Carlo sweeps are simulated in a single run. To simulate electric hysteresis, we apply an electric field along the [111] or [001] directions. The [111] field allows us to gain the understanding of how films respond to the electric field components along the directions that differ by symmetry, while the [001] field simulates the experimentally realizable setup.

To decouple contributions from the surface effects, depolarizing field, and epitaxial strain on the properties and phases of $PbZrO_3$ ultrathin films, we simulate different mechanical and electrical boundary conditions. Technically, mechanical boundary conditions are simulated by freezing some components of the strain tensor to model epitaxial strain in the range of -2% to 2%. [23]. To account for the electrical boundary conditions, we consider two limiting cases of surface charge compensation realized in experiments [24], namely ideal short-circuit and ideal open-circuit boundary conditions. Ideal short (open) circuit conditions model the situation when free carriers—intrinsic or extrinsic—are abundant (not available) to compensate potential polarization discontinuity at the film's surfaces. Technically, these conditions are simulated by either applying or removing periodic boundary conditions along the film's finite dimension when computing dipole-dipole interactions [25].

We begin by considering the effect of the surface on the properties of ultrathin $PbZrO_3$ films. For that, we carry out simulations for stress-free films of different thicknesses under either short-circuit or open-circuit boundary conditions. Figure 1(a) shows room temperature hysteresis loops computed for the films of different thicknesses under short circuit boundary conditions. The thickest film exhibits a double loop that is characteristic of an AFE behavior. As the film's thickness decreases, the loops begin to widen along the electric field axis and gradually transform into a single loop dependence that signifies the onset of a FE behavior. The 2.5 nm thick film exhibits a typical FE hysteresis loop. The size evolution of the hysteresis loops is in excellent qualitative agreement with experimental measurements [7–10,14]. A quantitative comparison is not always possible due to a difference in films' thicknesses in computations and experiments. We find a FE tetragonal phase in ultrathin $PbZrO_3$ films that is consistent with the experimental observation of ferroelectricity along the c axis (in orthorhombic notations) in $PbZrO_3$ films grown along the $(001)_O$ direction [14]. It should be noted that Ref. [9]

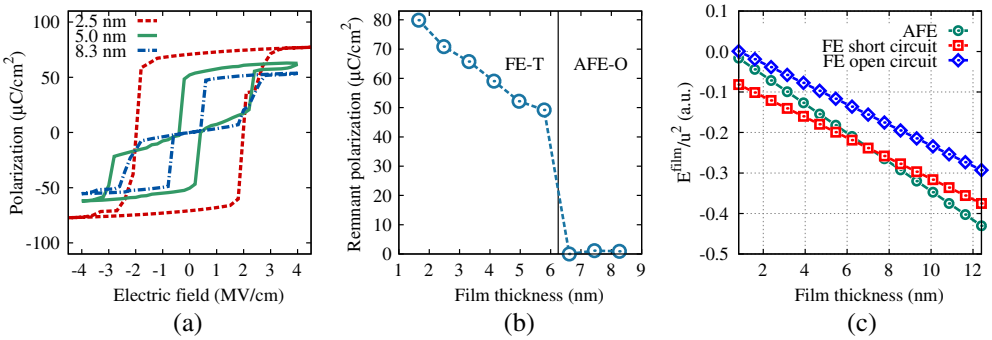

FIG. 1 (color online). Panel (a) gives the room temperature hysteresis loops for $PbZrO_3$ films of different thicknesses. The polarization is along the growth direction. The electric field is applied along the [111] direction. The data for the [001] field are given in [25]. Panel (b) shows the dependence of the remnant polarization on the film's thickness at room temperature. The solid vertical line indicates the boundary between FE tetragonal (FE-T) and AFE orthorhombic (AFE-O) phases. Panel (c) reports the dependence of the energy on the film's thickness computed using the reduced model described in the text. The model includes local mode self-energy, dipole-dipole, and short-range interactions between local modes. Different lines give the energy of the AFE or FE phases.

deduced a rhombohedral zero field phase for their thinnest epitaxial films. Figure 1(b) shows the dependence of the remnant polarization on the film's thickness. The data indicate that the remnant polarization first decreases as a function of the film's thickness in a qualitative agreement with experiment [9] and then disappears abruptly at the critical thickness of 6.5 nm. The latter finding is in excellent agreement with the experimental study that reported a FE phase for 6 nm thick $PbZrO_3$ layers [10]. An example of an electric hysteresis loop for a film under ideal open circuit conditions is given in [25]. Under such conditions, we do not find a size-driven onset of ferroelectricity due to a prohibitively large depolarizing field that would accompany a FE phase in the absence of screening charge.

The most striking finding is the size-driven onset of ferroelectricity in ultrathin $PbZrO_3$ films under short-circuit boundary conditions in the absence of epitaxial strain. This unexpected result cannot be explained by any ferroelectricity stabilizing mechanism proposed in the literature so far. We recall that the proposed mechanisms are mostly of extrinsic origin and include the presence of residual stresses and/or interfacial electrostatic effects. In contrast, the mechanism that stabilizes a FE phase in ultrathin films is rather of intrinsic origin as it is activated in the absence of an interface with a substrate. To reveal an atomistic origin of such an unusual effect, we investigate the interactions that are primarily responsible for the AFE behavior of $PbZrO_3$. They are the local mode self-energy, dipole-dipole, and short-range interactions between the local modes. While the self-energy ensures that the material undergoes structural distortions, it is the balance between the electrostatic dipole-dipole and short-range interactions that determines the actual type of the distortion, such as polar or antipolar, for example. Ferroelectricity, for instance, is stabilized by Coulomb interactions and destabilized by short-range interactions that arise from electronic hybridization and repulsion [15,27]. In $PbZrO_3$, the short-range interactions are dominated by a very strong repulsion between nearest neighbor dipoles with "head-to-tail" orientation of the dipole moments. This type of interaction is at least 1 order of magnitude stronger than any other type of short-range interaction in $PbZrO_3$ [17]. We, therefore, retain only this dominant interaction in order to simplify the discussion. In this approximation, the normalized energy per five atom cell in the FE tetragonal phase of bulk $PbZrO_3$ is $E_{\mathrm{FE}}^{\mathrm{bulk}}/u^2 = j_2 - 2.09(Z^{*2}/\varepsilon_\infty a_0^3)$, where the first and second terms give contributions from the short-range and dipole-dipole interactions, respectively. $j_2 = 0.024$ a.u. Z^*, ε_∞, and a_0 are Born effective charge, optical dielectric constant, and cubic lattice constant of $PbZrO_3$, respectively [17]. In the same approximation, the energy of an AFE orthorhombic phase associated with the distortion at the Σ_2 point of the Brillouin zone reduces to a sole contribution from the dipole-dipole interaction $E_{\mathrm{AFE}}^{\mathrm{bulk}}/u^2 = -0.53(Z^{*2}/\varepsilon_\infty a_0^3)$. Comparison of $E_{\mathrm{FE}}^{\mathrm{bulk}}$ and $E_{\mathrm{AFE}}^{\mathrm{bulk}}$ reveals that, in bulk $PbZrO_3$, the AFE phase develops in order to avoid the costly short-range interactions between head-to-tail dipoles. Next, we consider energies for a surface layer of dipoles in a film under ideal short circuit boundary conditions. They are $E_{\mathrm{FE}}^{\mathrm{surface}}/u^2 = -2.09(Z^{*2}/\varepsilon_\infty a_0^3)$ and $E_{\mathrm{AFE}}^{\mathrm{surface}}/u^2 = -0.53(Z^{*2}/\varepsilon_\infty a_0^3)$. It is now obvious that the presence of the surface favors the FE phase as it effectively removes the energetically costly interactions between head-to-tail dipoles. Interestingly, surface induced enhancement of ferroelectricity has been previously reported for ferroelectric ultrathin $PbTiO_3$ films under short-circuit boundary conditions [19]. Our model predicts that the FE phases are formed near the surface of $PbZrO_3$.

To further elucidate the existence of a critical thickness for antiferroelectricity in $PbZrO_3$ ultrathin films, we apply this reduced model to a film with N layers. Two of these layers are next to the top and bottom surfaces of the film. The corresponding energies for the FE and AFE phases are $E_{\mathrm{FE}}^{\mathrm{film}} = (N-2)E_{\mathrm{FE}}^{\mathrm{bulk}} + 2E_{\mathrm{FE}}^{\mathrm{surface}}$ and $E_{\mathrm{AFE}}^{\mathrm{film}} = (N-2)E_{\mathrm{AFE}}^{\mathrm{bulk}} + 2E_{\mathrm{AFE}}^{\mathrm{surface}}$, respectively. The difference between these two energies gives an estimate of the relative stability of FE and AFE phases at zero Kelvin. Figure 1(c) gives the dependencies of $E_{\mathrm{FE}}^{\mathrm{film}}/u^2$ and $E_{\mathrm{AFE}}^{\mathrm{film}}/u^2$ on the film's thickness computed without approximating short-range interactions with a single contribution from the nearest neighbors. The figure predicts that, at zero Kelvin, the energies of two phases become comparable at the critical thickness of 7 nm in excellent agreement with the room temperature calculations reported in Fig. 1(b) and the experimental findings of Ref. [10]. Below this critical thickness, the FE tetragonal phase is energetically more favorable. This finding allows us to conclude that, in $PbZrO_3$ ultrathin films, the FE phase is stabilized by the surface that eliminates energetically costly short-range interactions between the neighboring dipoles. The stability of the FE phase increases with the increase in the surface to volume ratio. Interestingly, such a finding could explain the increase in the critical thickness in fine grain polycrystalline films [8] as compared to the single crystalline ones [9]. It also suggests that the effect could be even more pronounced in other low-dimensional structures, such as nanorods and nanodots, as they have a larger surface to volume ratio. Our computations reveal the crucial role of the surface in stabilizing the FE phase in $PbZrO_3$ nanostructures beyond the epitaxial strain and interfacial effects. Such an intrinsic mechanism aids in the understanding of ferroelectricity onset in nanostructures where residual stresses do not contribute significantly [7].

Figure 1(c) also reports energy estimates for the FE phase developed in ultrathin films under ideal open-circuit boundary conditions. In agreement with our computational findings, the energy analysis demonstrates that, under such conditions, the AFE phase remains energetically more

favorable for any thickness. Interestingly, the presence of free carriers which provide only partial surface charge compensation in a FE phase is expected to produce energy dependencies which fall in between the lines for the ideal short- and open-circuit boundary conditions [see Fig. 1(c)]. Many of these dependencies will cross the AFE phase energy to give rise to the size-driven AFE-FE transition. However, the energy gain due to the FE phase formation will be less as compared to the case of full surface charge compensation and will result in a lower transition temperature and reduced critical thickness.

Interestingly, Fig. 1(c) further predicts that, in the vicinity of the critical thickness, the AFE and FE phases are very close in energy. This suggests that the AFE-FE phase transition in AFE nanostructures can be achieved with lower electric fields as compared to the bulk. Furthermore, this field is expected to decrease with the film's thickness. The energetic proximity of AFE and FE phases also implies a phase competition that is likely to result in phase coexistence. Indeed, such coexistence was reported experimentally [9,14]. The phase competition and the energy balance is expected to be affected by the temperature so that different phases are stabilized at different temperatures. To verify this, we carried out finite-temperature simulations for a 5 nm thick film that has mixed AFE-FE behavior under electric field (see Fig. 1). Figs. 2(a)–2(c) show computational data from the annealing simulations that started at 1200 K and proceeded in steps of 10 K decrements. The data indicate a single transition into an AFE orthorhombic phase at 780 K that is below the computational transition temperature of 946 K for bulk $PbZrO_3$. At the same time, the zero Kelvin analysis [see Fig. 1(c)] and electric field simulations [see Figs. 1(a) and 1(b)] suggest a FE phase below 300 K. To investigate this controversy, we carried out a slow heating simulation from the FE ground state. The results are given in Figs. 2(d)–2(f) and show an abrupt transition from a FE to an AFE phase at 380 K. The dramatic difference between the results from annealing and heating simulations confirms that there exists a phase competition that results in the stabilization of a FE phase at lower temperatures and an AFE phase at higher temperatures. This can be tentatively attributed to the larger entropy associated with the AFE phase. The computational finding of the AFE to FE phase transition at 380 K is in qualitative agreement with the experimental result of Ref. [14] where the FE phase was found to be stable below 60 K, while the AFE is stabilized above this temperature. The fact that the computational transition temperature is higher than the experimental one is attributed to the fact that the experimental films are likely to be under partial surface charge compensation rather than the full compensation simulated here as well as the fact that our computational method overestimates the transition temperature of bulk $PbZrO_3$.

Next, we turn to the effect of epitaxial strain on the electric properties and phase competition in $PbZrO_3$

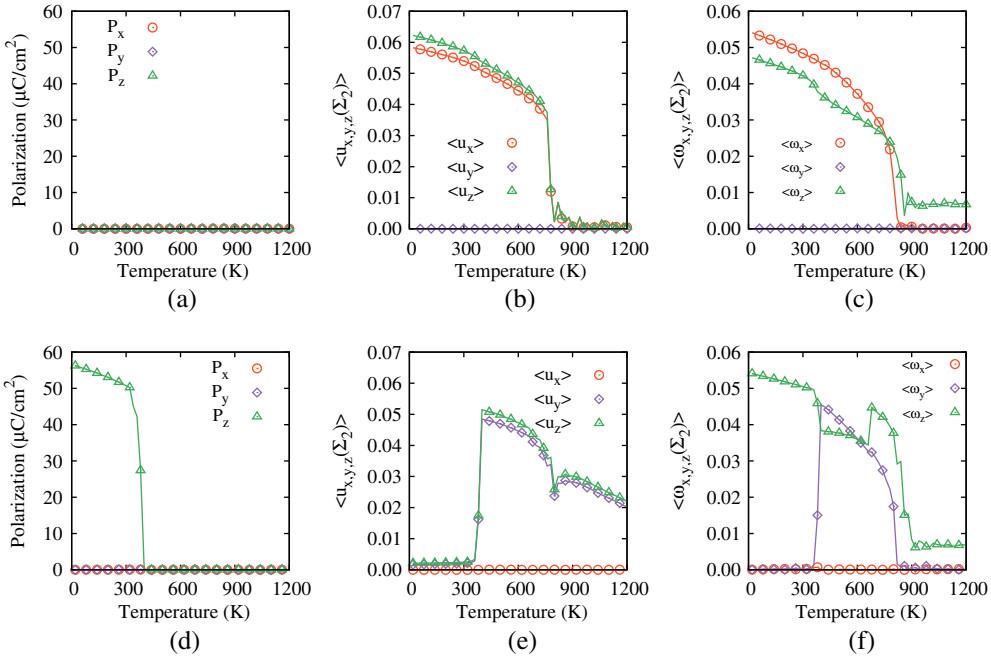

FIG. 2 (color online). Temperature dependencies of order parameters in 5 nm thick film. Panels (a)–(c) give the results from annealing simulations. Panels (d)–(f) present the data of heating simulations from the tetragonal ground state. $P_{x,y,z}$ give the polarization components, $\langle u_{x,y,z}(\Sigma_2)\rangle$ give the components of the AFE order parameter at the Σ_2 point of the Brillouin zone, while $\langle \omega_{x,y,z}\rangle$ give the components of the order parameter associated with antiferrodistortive tilts of oxygen octahedra. The order parameters are reported in units of cubic lattice constant of $PbZrO_3$, $a_0 = 7.81$ a.u.

ultrathin films. Our computational data [25] suggest that, in agreement with zero Kelvin first principles calculations [11] and experimental findings [9,10,14], compressive strain further stabilizes the FE phase. Tensile strain favors the AFE phase. Under tensile strain, we do not observe any polarization along the film's growth direction. Under ideal open-circuit boundary conditions, we find the AFE zero-field phase for all strains considered.

In summary, we have predicted the existence of a critical thickness for antiferroelectricity in ultrathin $PbZrO_3$ films. Below this critical thickness, the films develop a FE tetragonal phase under ideal short-circuit boundary conditions. The origin of this size-driven AFE-FE phase transition is traced to the intrinsic surface effect that stabilizes the FE phase by removing energetically costly short-range interactions between head-to-tail dipoles. The energy gain due to FE phase formation increases with the increase in surface to bulk ratio. The existence of the critical thickness for antiferroelectricity below which the AFE-FE transition occurs complements the earlier discovery of critical thickness for ferroelectricity [2] below which the single domain FE phase breaks into nanodomains that can behave like an AFE-like phase. Such antisymmetry between ferroelectrics and antiferroelectrics upon scaling down suggests that ferroelectricity and antiferroelectricity are just two opposite manifestations of the same phenomenon: the material's tendency to develop a long-range order. This Letter provides insights into previously overlooked surface effects as well as a comprehensive view of the role that electrical and mechanical boundary conditions play in phase formation in AFE ultrathin films. We believe that it will stimulate further research in the area of functional nanoscale materials.

The present work is supported by the U.S. Department of Energy, Office of Basic Energy Sciences, Division of Materials Sciences and Engineering under Grant No. DE-SC0005245. This research used resources of the National Energy Research Scientific Computing Center, which is supported by the Office of Science of the U.S. Department of Energy under Contract No. DE-AC02-05CH11231.

[1] C. Lichtensteiger, M. Dawber, and J. Triscone, in *Physics of Ferroelectrics: A Modern Perspective*, edited by K. Rabe, C. Ahn, and J.-M. Triscone, eds., (Springer, New York, 2007), pp. 305–338.
[2] J. Junquera and P. Ghosez, Nature (London) **422**, 506 (2003).
[3] D. D. Fong, G. B. Stephenson, S. K. Streiffer, J. A. Eastman, O. Auciello, P. H. Fuoss, and C. Thompson, Science **304**, 1650 (2004).
[4] S. K. Streiffer, J. A. Eastman, D. D. Fong, C. Thompson, A. Munkholm, M. V. Ramana Murty, O. Auciello, G. R. Bai, and G. B. Stephenson, Phys. Rev. Lett. **89**, 067601 (2002).
[5] P. Zubko, N. Jecklin, N. Stucki, C. Lichtensteiger, G. Rispens, and J.-M. Triscone, Ferroelectrics **433**, 127 (2012).
[6] E. Glazkova, K. McCash, C.-M. Chang, B. K. Mani, and I. Ponomareva, Appl. Phys. Lett. **104**, 012909 (2014).
[7] P. Ayyub, S. Chattopadhyay, R. Pinto, and M. S. Multani, Phys. Rev. B **57**, R5559 (1998).
[8] J. Zhai, Y. Yao, X. Li, T. F. Hung, Z. K. Xu, H. Chen, E. V. Colla, and T. B. Wu, J. Appl. Phys. **92**, 3990 (2002).
[9] A. Roy Chaudhuri, M. Arredondo, A. Hähnel, A. Morelli, M. Becker, M. Alexe, and I. Vrejoiu, Phys. Rev. B **84**, 054112 (2011).
[10] K. Boldyreva, L. Pintilie, A. Lotnyk, I. B. Misirlioglu, M. Alexe, and D. Hesse, Appl. Phys. Lett. **91**, 122915 (2007).
[11] S. E. Reyes-Lillo and K. M. Rabe, Phys. Rev. B **88**, 180102 (2013).
[12] I. Kornev, H. Fu, and L. Bellaiche, Phys. Rev. Lett. **93**, 196104 (2004).
[13] I. Ponomareva and L. Bellaiche, Phys. Rev. B **74**, 064102 (2006).
[14] L. Pintilie, K. Boldyreva, M. Alexe, and D. Hesse, J. Appl. Phys. **103**, 024101 (2008).
[15] W. Zhong, D. Vanderbilt, and K. M. Rabe, Phys. Rev. B **52**, 6301 (1995).
[16] D. Vanderbilt and W. Zhong, Ferroelectrics **206**, 181 (1998).
[17] B. K. Mani, S. Lisenkov, and I. Ponomareva, Phys. Rev. B **91**, 134112 (2015).
[18] L. Bellaiche, A. Garcia, and D. Vanderbilt, Phys. Rev. Lett. **84**, 5427 (2000).
[19] P. Ghosez and K. M. Rabe, Appl. Phys. Lett. **76**, 2767 (2000).
[20] I. I. Naumov, L. Bellaiche, and H. Fu, Nature (London) **432**, 737 (2004).
[21] N. Choudhury, L. Walizer, S. Lisenkov, and L. Bellaiche, Nature (London) **470**, 513 (2011).
[22] S. Bhattacharjee, D. Rahmedov, D. Wang, J. Íñiguez, and L. Bellaiche, Phys. Rev. Lett. **112**, 147601 (2014).
[23] Negative (positive) strains correspond to epitaxial compression (tension).
[24] M. J. Highland, T. T. Fister, D. D. Fong, P. H. Fuoss, C. Thompson, J. A. Eastman, S. K. Streiffer, and G. B. Stephenson, Phys. Rev. Lett. **107**, 187602 (2011).
[25] See Supplemental Material at http://link.aps.org/supplemental/10.1103/PhysRevLett.115.097601 for the technical details regarding modeling of ideal short circuit and open circuit boundary conditions, the effect of epitaxial strain, and the data for the films under electric field applied along [001] direction, which includes Ref. [26].
[26] I. Ponomareva, I. I. Naumov, I. Kornev, H. Fu, and L. Bellaiche, Phys. Rev. B **72**, 140102 (2005).
[27] W. Cochran, Phys. Rev. Lett. **3**, 412 (1959).